CROATICA CHEMICA ACTA
CCACAA **77** (3) 457–464 (2004)
ISSN-0011-1643
CCA-2947
Original Scientific Paper

C_{70} Dimers – Energetics and Topology

Csaba L. Nagy,[a] Monica Stefu,[a] Mircea V. Diudea,[b,*] Andreas Dress,[b] and Achim Müller[c]

[a]*Faculty of Chemistry and Chemical Engineering, Babes-Bolyai University, 400 084 Cluj, Romania*
[b]*Fakultät für Mathematik, Universität Bielefeld, D-33615 Bielefeld, Germany*
[c]*Fakultät für Chemie, Universität Bielefeld, D-33615 Bielefeld, Germany*

RECEIVED JUNE 20, 2003; REVISED SEPTEMBER 30, 2003; ACCEPTED SEPTEMBER 30, 2003

Key words
dimeric fullerenes
sp^3 adducts
sp^2 dimers
sp^2 tubulene
C_{70}-peanut dimers
dimer topology

All sp^2 peanut-shaped dimeric fullerenes derived from D_{5h} C_{70} are modeled. Construction of the isomers was monitored by a cyclic permutation of bonds in the linking zone of the two caps resulting from deleting the boundary of a face from the parent C_{70} fullerene. Local curvature was calculated in terms of both angular defects and strain energy. Topological equivalence classes of the constituent substructures were evaluated by calculating the topological indices of the parent cages, their medials and duals. Detailed network transformation, starting from C_{70}, through sp^3 dimer, peanut sp^2 dimer, up to the corresponding tubulene is given. Semiempirical calculations showed a monotonic decrease in the heat of formation along the above pathway.

INTRODUCTION

The discovery of fullerenes, nanotubes and other novel allotropic forms of carbon has generated a research explosion in the fields of chemistry, physics, and materials science. The initial fascinating appeal, coming from their beautiful symmetry[1–3] was later shifted to real chemistry.[4–6] Carbon allotropes with finite molecular cage structures have been functionalized or inserted in supramolecular assemblies.[7,8] A fullerene is an all-carbon molecule in which the atoms are arranged in a pseudospherical framework made up entirely of pentagons and hexagons. »Non-classical« extensions to include rings of other sizes have been considered.[9,10] Multielemental cages containing pentagons and hexagons have also been studied.[11]

Dimeric fullerenes like C_{120} and C_{140} have been reported in literature as a result of a [2+2] cap-to-cap cycloaddition.[12–14] In the attributed structures, the two cages are linked *via* a four-fold ring, consisting of sp^3 hybridized carbon atoms. Linear chains of spherical monomers (C_{60}), formed at moderate pressure (1 GPa) and 300 °C have also been reported.[12] A different molecular structure, with a peanut-shape and all sp^2 carbon atoms, has been proposed as well.[15–17]

The present paper deals with the construction of all distinct sp^2 peanut dimers of D_{5h} C_{70}. The topological characterization of these objects, including local curvature and subgraph equivalence classes calculation, is presented in the next section. The energy diagram of the detailed network transformation starting from the monomer, through a peanut dimer up to the corresponding tubulene, is given in terms of semiempirical data, in the third section.

sp^3 ADDUCTS

Dimeric fullerenes such as C_{120}, C_{140}, and the mixed C_{130} have been synthesized.[18] The attributed structures involve

* Author to whom correspondence should be addressed. (E-mail: diudea@chem.ubbcluj.ro)

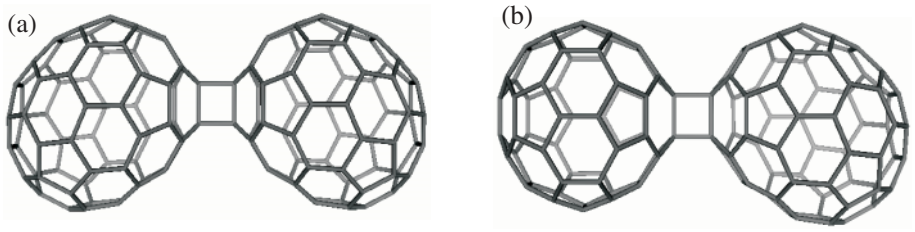

Figure 1. The most stable sp^3 C_{140} (a) and C_{130} (b) dimers.

sp^3 hybridized carbon atoms (Figure 1) and are supposed to result from a [2+2] cycloaddition.

The most stable structure is that of a [6,6] adduct. However, in the further isomerization process (see below), the appearing pentagon pairs (pentalene units) will undesirably raise the barrier energy. In such a transformation, the sp^3 [5,6]-*trans* adduct is prone.

sp^2 DIMERS

A tubulene is defined as a capped nanotube built up of two hemifullerene caps and a distancing tube portion. Various caps can be derived from a fullerene by deleting one or more faces. Subsequently, various tubulene-like objects can be imagined, some of them appearing as intermediates in the coalescence reaction of spherical fullerenes (see below), ending with a tubulene.

Take a fullerene face and delete the bonds forming its boundary. This results in an open structure with dangling bonds (*i.e.*, with monovalent terminal atoms). Put two such objects face to face and join each single-connected atom of the first structure with its corresponding atom and the next atom in the second structure. In this way an all sp^2 peanut-shaped dimer is obtained.

There are five topologically distinct faces in C_{70} (Figure 2a – two pentagons and three hexagons), which supply five caps (Figure 2b–f, dangling bonds are not shown).

The junction zone is tessellated by either pure heptagons (caps a and c) or heptagons and hexagons (caps b, d and e) according to the cap topology.

No mixed dimers C_{60}–C_{70} were constructed. Figure 3 illustrates the *in silico* building of dimer C_{140}ef. It could appear in the coalescence of two quasi-spherical C_{70} molecules (see below). Note that the procedure in Figure 3 is useful for straight modeling of a peanut dimer.

Construction of all possible C_{70}-peanut dimers was monitored by a cyclic permutation on the sequence of edges in the joining zone (Table I). The sequence designated by a single letter represents the fixed cap, while the others (denoted by two letters) correspond to the rotated cap. The start of the sequence is given in boldface.

Several enantiomer pairs appear among the dimers shown in Table I (Table II). Two enantiomers have the same edge sequence but a different circular visiting sense. They have identical topological and energetic parameters, thus leaving only twelve distinct dimeric structures (see the next section).

The lattice transformation of two C_{70} fullerenes passing through the peanut dimer up to the corresponding tubulene (Figure 4) is presented in Figure 5 as geodesic projections.

Two facing pentagons rotated by $\pi/5$ (Figure 5a) are connected by two bonds, thus introducing sp^3 hybridization (Figure 5b, bold lines). In order to recover the sp^2 network, one bond in each sphere will break (Figure 5b,

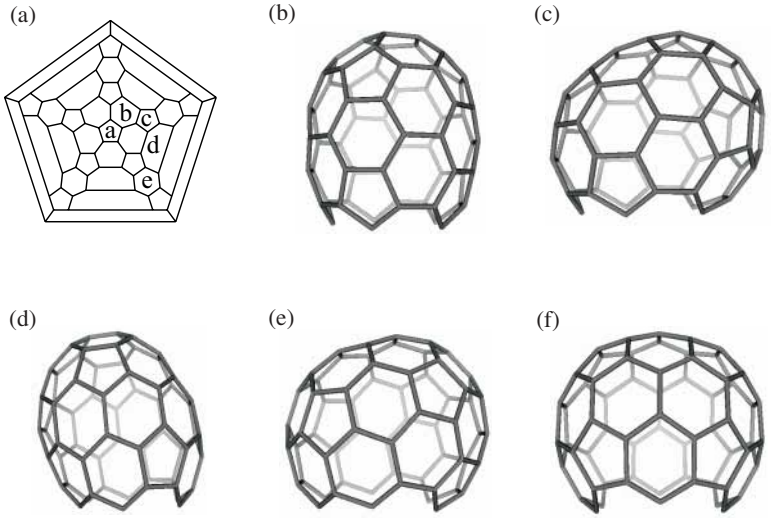

Figure 2. Scheme of ring labeling in C_{70} and the possible 5 caps. (a) Schlegel projection of C_{70}, (b) cap a, (c) cap b, (d) cap c, (e) cap d, (f) cap e.

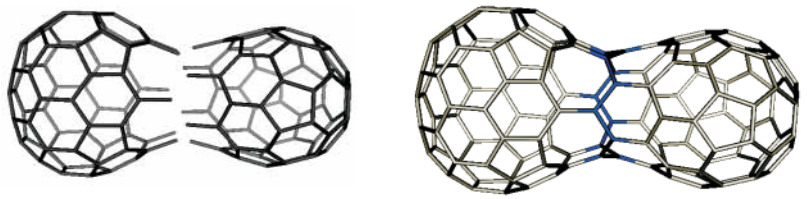

Figure 3. Construction of the C_{140}ef dimer.

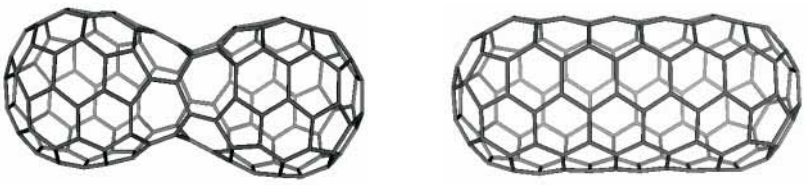

Figure 4. The C_{140}aa peanut dimer and its corresponding tubulene.

TABLE I. Edge typing of the constructed sp^2 dimers

G	Edge typing
a	57 57 67 57 57 67 57 57 67 57 57 67 57 57 67
aa	57 67 57 57 67 57 57 67 57 57 67 57 57 67 57
b	57 67 66 66 67 57 67 66 66 67 67 67 66 66 67
bb	67 **66** 66 67 57 67 66 66 67 67 67 66 66 67 57
bc	67 66 66 67 67 67 **66** 66 67 57 67 66 66 67 57
bd	67 66 66 67 57 67 66 66 67 57 67 **66** 66 67 67
be	66 67 57 **67** 66 66 67 67 67 66 66 67 57 67 66
bf	66 67 57 67 66 66 67 57 67 66 66 67 67 **67** 66
bg	66 67 67 67 66 66 67 57 **67** 66 66 67 57 67 66
c	57 57 67 57 57 67 57 57 67 67 67 57 67 67 67
cc	67 57 **57** 67 57 57 67 67 67 57 67 67 67 57 57
cd	67 57 57 67 67 **67** 57 67 67 67 57 57 67 57 57
ce	67 67 67 57 67 67 67 57 **57** 67 57 57 67 57 57
cf	67 57 67 67 67 57 57 67 57 57 **67** 57 57 67 67
cg	67 57 57 67 57 57 67 57 57 67 67 67 57 67 **67**
d	57 57 67 57 57 67 67 66 66 67 57 67 66 66 67 67
dd	67 57 57 67 57 57 67 67 66 66 67 57 67 66 66 **67**
de	66 66 67 67 57 57 67 57 57 67 67 66 **66** 67 57 67
df	67 57 67 66 66 67 67 57 57 **67** 57 57 67 67 66 66
dg	66 66 67 57 67 66 66 **67** 67 57 57 67 57 57 67 67
dh	67 67 66 66 67 **57** 67 66 66 67 67 57 57 67 57 57
di	67 57 **57** 67 67 66 66 67 57 67 66 66 67 67 57 57
e	66 67 57 67 67 57 67 66 66 67 57 67 67 57 67 66
ee	66 66 67 57 67 67 57 **67** 66 66 67 57 67 67 57 **67**
ef	67 57 67 66 **66** 67 57 67 67 57 67 66 **66** 67 57 67
eg	67 **57** 67 67 57 67 66 66 67 **57** 67 67 57 67 66 66

TABLE II. Enantiomer pairs of the peanut dimers

G	bf	bg	be	cg	cf	di	dh	dg	eg
Enantiomer pair	bb	bc	bd	cc	cd	dd	de	df	ee

thick dotted lines) and undergo Stone-Wales rotation[19] (Figure 5c); the linking zone now consists of two H-shaped bridges, with four heptagons and two nonagons (Figure 5d). The peanut-shaped structure will be achieved in four SW steps, performed along the circumference (Figure 5d, bold lines) while the junction zone becomes covered by heptagons (Figure 5e). This induces a negative curvature strain, but it is relaxed once the heptagons and adjacent pentagons are transformed into a hexagonal lattice (Figure 5f). For this, ten SW steps are necessary in a circumferential order (Figure 5e, bold lines).

The energy involved in the coalescence process is presented in Figure 6.

DIMER TOPOLOGY

Dimer Curvature

Let G = G (*V*, *E*) be a connected graph with the vertex set $V = V$ (G), and edge set $E = E$ (G). Map M is the combinatorial representation of a closed surface. If the graph G is a cycle-containing one, it can superimpose on M. Consequently, one can define $F = F$(G) as the set of graph faces (*i.e.*, closed regions). Denote the cardinality of the above sets by *v*, *e* and *f*.

Combinatorial topology of fullerenes can be described by the Euler theorem:[20]

$$v - e + f = \chi(S) = 2(1 - g) \qquad (1)$$

where χ is the Euler characteristic, and *g* is the genus of the graph ($g = 0$ for a graph embedded in the sphere, and 1 in case of a torus). This formula is useful for checking the consistency of an assumed structure.

According to the Gauss-Bonnet theorem, the total Gaussian curvature *k* on a surface *S* represents a topological invariant:[21]

$$\int_S k dA = 2\pi\chi(S) \qquad (2)$$

An angular defect (or excess) at a vertex *u* takes into account the contributions (on average) of the surrounding

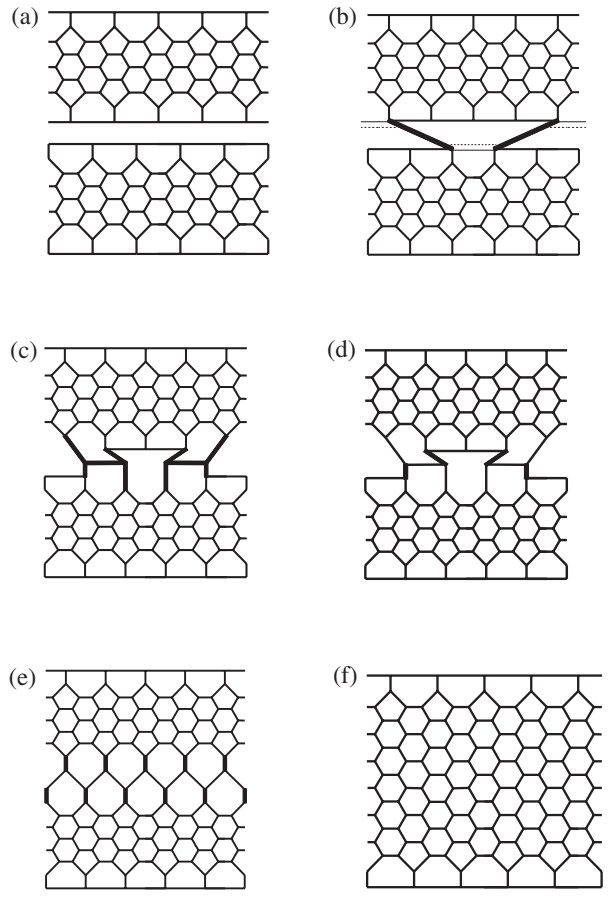

Figure 5. Geodesic projections of the coalescence steps.

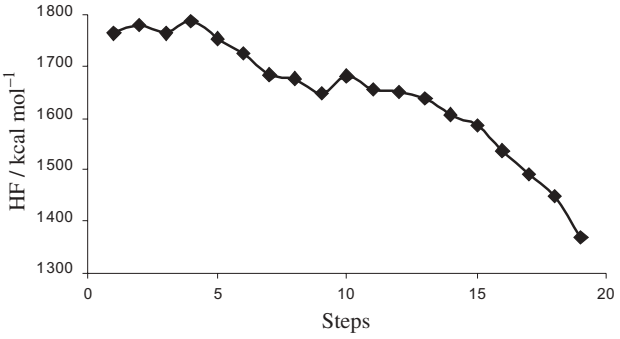

Figure 6. Energy curve for the coalescence pathway of 2 × C_{70}.

faces, keeping in mind that the sum of angles of any face (*i.e.*, polygon) f_j is $(j - 2)\pi$:

$$s(u) = \pi \sum_j \frac{j-2}{j} \tag{3}$$

Since the total angular area surrounding a point u on a smooth surface is 2π, it is convenient to define the angular defect (a combinatorial curvature) as:

$$ad(u) = 2 - s(u) / \pi \tag{4}$$

The total angular defect for a given combinatorial surface can be calculated by:

$$ad(P) = \sum_u ad(u) \tag{5}$$

Euler's theorem (1) can be rephrased in terms of angular defects, stating that $ad(P)$, taken over all vertices of a polyhedron P, is quite independent of the specific structure of the polyhedron: always equal to 4 if the polyhedron is embedded in the sphere, implying that enough vertices of positive angular defect must exist in any spherical polyhedron. In the case of a polyhedron embedded in the torus or in the tube, the corresponding version of Euler's theorem states that the sum of its angular defects must always vanish (see Eqs. (1) and (2)). Further, this sum is negative for every polyhedron of a negative Euler characteristic.

In order to describe the local curvature, we selected a zone of two rows of faces each hand to the equator (*i.e.*, the ring joining the two caps). Next, we made »longitudinal« selections (Figure 7, in bold line) within the above »parallel« selection up to complete circumscription of the structure. The local curvature was calculated (by CageVersatile v.1.1,[22]) according to Eqs. (3) to (5).

The curvature in the parallel selection is a characteristic of each of the five classes of dimers. The values are as follows: class a, 0.00; class b, 0.533; class c, 0.667; class d, 0.933 and class e, 0.80. All of them have positive signs despite the saddle-type geometry, thus being less informative. The total curvature for all constructed dimers was 4 (see above).

As mentioned above, the curvature of a selection sequence is proper for a given dimer. In the case of enantiomer pairs, the same sequence of curvature is expected but the visiting sense is opposite. Table III presents the values for these selections, the start in a circumscribing longitudinal sequence being given in boldface.

The local negative curvature is reflected in the sign of curvature values in Table III. It can be viewed as the fingerprint of a structure.

Strain Energy Calculation

In the POAV1 theory,[23–26] the π-orbital axis vector is defined as the vector that makes equal angles $\theta_{\sigma\pi}$ to the three σ-bonds of the sp^2 carbon atom and the pyramidalization angle is obtained as:

$$\theta_p = \theta_{\sigma\pi} - 90° \tag{6}$$

This angle is used for estimating the strain energy, induced by a pyramidalized carbon atom, by:

$$E_s = 200 \cdot (\theta_p)^2 \tag{7}$$

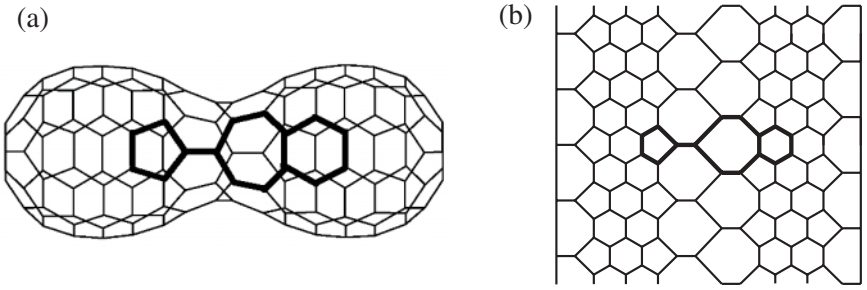

Figure 7. Selections for local curvature evaluation in the C_{140}aa dimer: (a) longitudinal selection, (b) geodesic projection of the selection.

TABLE III. Curvature values of the longitudinal selections

G	S_1	S_2	S_3	S_4	S_5	S_6	S_7	S_8	S_9	S_{10}	S_{11}	S_{12}
aa	**–0.171**	–0.171	–0.171	–0.171	–0.171	–0.171	–0.171	–0.171	–0.171	–0.171		
bb	**–0.057**	–0.248	–0.248	–0.124	–0.124	–0.248	–0.248	–0.057	0.076	–0.048	–0.048	0.076
bc	**–0.057**	–0.248	–0.248	–0.057	0.010	–0.181	–0.114	–0.057	–0.057	–0.114	–0.181	0.010
bd	**0.076**	–0.181	–0.114	–0.057	–0.124	–0.248	–0.248	–0.124	–0.057	–0.114	–0.181	0.076
cc	**–0.238**	–0.305	–0.305	–0.305	–0.305	–0.238	–0.038	–0.038	–0.038	–0.038		
cd	**–0.238**	–0.305	–0.305	–0.238	–0.105	–0.238	–0.038	–0.038	–0.238	–0.105		
ce	**–0.238**	–0.105	–0.238	–0.105	–0.238	–0.238	–0.105	–0.238	–0.105	–0.238		
dd	**–0.143**	–0.038	–0.038	–0.143	–0.152	–0.181	–0.048	0.076	0.076	–0.048	–0.181	–0.152
de	**–0.171**	–0.048	–0.143	–0.143	–0.048	–0.171	–0.019	–0.057	–0.048	–0.048	–0.057	–0.019
df	**–0.048**	0.086	–0.171	–0.152	–0.152	–0.171	0.086	–0.048	–0.019	–0.181	–0.181	–0.019
ee	**–0.019**	–0.210	–0.210	–0.019	–0.048	–0.048	–0.019	–0.210	–0.210	–0.019	–0.048	–0.048
ef	**–0.019**	–0.238	–0.019	–0.019	–0.238	–0.019	–0.019	–0.238	–0.019	–0.019	–0.238	–0.019
						Enantiomer pairs as presented in Table II						
bf	0.076	–0.057	–0.248	–0.248	–0.124	–0.124	–0.248	–0.248	**–0.057**	0.076	–0.048	–0.048
bg	–0.057	–0.057	–0.114	–0.181	0.010	–0.057	–0.248	–0.248	**–0.057**	0.010	–0.181	–0.114
be	–0.057	–0.124	–0.248	–0.248	–0.124	–0.057	–0.114	–0.181	**0.076**	0.076	–0.181	–0.114
cg	–0.038	–0.238	–0.305	–0.305	–0.305	–0.305	**–0.238**	–0.038	–0.038	–0.038		
cf	–0.038	–0.238	–0.105	–0.238	–0.305	–0.305	**–0.238**	–0.105	–0.238	–0.038		
di	–0.038	–0.038	**–0.143**	–0.152	–0.181	–0.048	0.076	0.076	–0.048	–0.181	–0.152	–0.143
dh	–0.143	–0.048	**–0.171**	–0.019	–0.057	–0.048	–0.048	–0.057	–0.019	–0.171	–0.048	–0.143
dg	–0.171	0.086	**–0.048**	–0.019	–0.181	–0.181	–0.019	–0.048	0.086	–0.171	–0.152	–0.152
eg	–0.210	–0.210	**–0.019**	–0.048	–0.048	–0.019	–0.210	–0.210	–0.019	–0.048	–0.048	–0.019

with θ_p being measured in radians. The difference $120 - \frac{1}{3}\sum\theta_p$ gives the deviation to planarity. Data of the POAV1 analysis for $D_{5h}C_{70}$, the peanut dimer and the corresponding tubulene are given in Table IV.

The results of the POAV1 analysis are in agreement with the heat of formation values (see Figure 6). The strain energy of the sp^3 adduct can be approximated as twice that of C_{70} (1010.388 kcal mol^{-1}). In the peanut structure, the vertices shared by three heptagons are only slightly deviated from planarity; however, the structure is still more strained than the corresponding tubulene. A negative value was attributed to the strain of atoms in the junction zone (level 8 and 9, Table IV) where the local curvature is negative. The tubulene is the most relaxed structure, as indicated by the lowest value of its total strain energy.

Topological Symmetry

Given a graph G with S = S(G) being the set of subgraphs of a given size and a group of automorphisms *Aut*(G(S)), the two subgraphs S_i, S_j of G are called equivalent if there is a group element $aut(N_{S_i}) \in Aut(G(S))$ such that $S_j\, aut(N_{S_i})\, S_i$ (*i.e.*, an automorphic permutation that transforms two subgraphs to each other).

The set of all subgraphs S_j obeying the above equivalence relation is called the orbit (*i.e.*, class of equivalence) of the subgraph S_i, $S_{N_{S_i}}$. The orbits represent disjoint automorphic partitions: $S = \cup S_{N_{S_i}}$. Our only object

TABLE IV. Data of the POAV1 analysis

Atom		Angle / deg			Deviation / deg	θ_p / deg	E_s / kcal mol^{-1}
Level	No.	1	2	3			
				C_{70}			
1	10	108.0	119.707	119.713	12.58	11.931	8.672
2	10	106.964	120.205	120.199	12.632	11.942	8.688
3	20	108.394	119.684	120.084	11.838	11.564	8.146
4	20	108.128	121.521	121.372	8.979	10.018	6.114
5	10	115.7	118.762	118.758	6.78	8.725	4.638
Total							505.194
				C_{140} peanut			
1	10	119.73	119.732	107.997	12.541	11.911	8.644
2	10	107.01	120.171	120.169	12.65	11.952	8.702
3	20	108.304	119.668	120.095	11.933	11.611	8.213
4	20	108.197	121.261	121.213	9.329	10.218	6.361
5	20	116.34	118.928	117.780	6.952	8.839	4.759
6	20	108.228	122.963	121.321	7.488	9.124	5.072
7	20	118.824	125.405	108.291	7.48	9.108	5.054
8	10	104.77	126.623	126.614	–1.993	4.633	1.308
9	10	122.641	114.01	122.64	–0.709	2.792	0.475
Total							744.828
				C_{140} tubulene			
1	10	119.762	119.761	108.001	12.476	11.879	8.597
2	10	106.867	120.128	120.124	12.881	12.063	8.865
3	20	108.5	120.11	119.125	12.265	11.78	8.454
4	20	108.069	122.113	120.31	9.508	10.317	6.484
5	20	117.604	118.65	118.453	5.293	7.696	3.608
6	20	118.453	120.225	118.462	2.86	5.638	1.936
7	20	119.3	119.004	119.16	2.536	5.307	1.716
8	20	119.37	118.294	118.716	3.62	6.35	2.456
Total							667.713

here is to find the equivalence classes for the vertices, edges and faces of a fullerene cage. As an equivalence criterion, we used the topological indices of centricity $C(LM)$ and centrocomplexity $X(LM)$, defined on layer matrices $\boldsymbol{LM}$.[27]

The vertex orbits are found by simply applying the above centric index to the layer of distance sum matrix $\boldsymbol{LDS}$ of the parent graph. The edge orbits are calculable with the same index but applied to the $\boldsymbol{LDS}$ matrix of the corresponding medial graph.[28]

The face orbits are obtained from the dual of the parent graph,[28] the criterion being the index of centrocomplexity $X(L^1W)$, where $\boldsymbol{L}^1\boldsymbol{W}$ matrix is the layer matrix of valences. Each vertex in the dual has the valence equal to the parent face size. In this way, one can select the orbits for each face type. Data are listed in Table V.

It can be seen that highly symmetric structures have a low number of equivalence classes.

Figure 8 illustrates the medial (Figure 8a) and the dual (Figure 8b) of the C_{140}aa dimer.

ENERGETICS OF C_{70}-PEANUT DIMERS

Molecular modeling was performed using the semiempirical method PM3 with the parametrization supplied by the HyperChem software (version 4.5, Hypercube, Inc.).[29] Structures were optimized using the Polak-Ribier conjugate-gradient method, energy minimization was terminated at an RMS gradient <0.01 kcal Å^{-1} mol^{-1} for all isomers.

The lowest heat of formation was computed for isomer aa (D_{5d} symmetry), for which the lowest deviation to

TABLE V. Subgraph equivalence classes in peanut C_{140} dimers

G	Vertices	Edges	Faces
c140aa	4x{10};5x{20};	9x{10};6x{20};	[5] 1{2}; 2{10}; [6] 4{10}; [7] 1{10};
c140bb	64x{2};3x{4};	2x{1};102x{2};1x{4};	[5] 3{2}; 3{4}; [6] 10{2}; 7{4}; [7] 1{2}; 1{4};
c140bc	66x{2};2x{4};	2x{1};87x{2};7x{4};1x{6};	[5] 3{2}; 3{4}; [6] 7{2}; 7{4}; 1{6}; [7] 3{2};
c140bd	70x{2};	2x{1};96x{2};4x{4};	[5] 3{2}; 3{4}; [6] 10{2}; 7{4}; [7] 3{2};
c140cc	66x{2};2x{4};	2x{1};94x{2};5x{4};	[5] 3{2}; 4{4}; [6] 1{2}; 8{4}; 1{6}; [7] 3{2}; 1{4};
c140cd	66x{2};2x{4};	2x{1};100x{2};2x{4};	[5] 3{2}; 4{4}; [6] 1{2}; 8{4}; 1{6}; [7] 1{2}; 2{4};
c140ce	4x{2};33x{4};	9x{2};48x{4};	[5] 3{2}; 4{4}; [6] 1{2}; 8{4}; 1{6}; [7] 1{2}; 2{4};
c140dd	68x{2};1x{4};	2x{1};104x{2};	[5] 8{2}; 1{4}; [6] 9{2}; 5{4}; 1{6}; [7] 2{2}; 1{4};
c140de	68x{2};1x{4};	2x{1};98x{2};3x{4};	[5] 6{2}; 2{4}; [6] 10{2}; 4{4}; 1{8}; [7] 4{2};
c140df	70x{2};	2x{1};102x{2};1x{4};	[5] 6{2}; 2{4}; [6] 9{2}; 5{4}; 1{6}; [7] 1{2}; 1{6};
c140ee	35x{4};	3x{2};45x{4};3x{8};	[5] 3{4}; 1{8}; [6] 5{4}; 3{8}; [7] 2{4};
c140ef	7x{4};14x{8};	1x{2};6x{4};23x{8};	[5] 1{4}; 2{8}; [6] 5{4}; 3{8}; [7] 1{8};

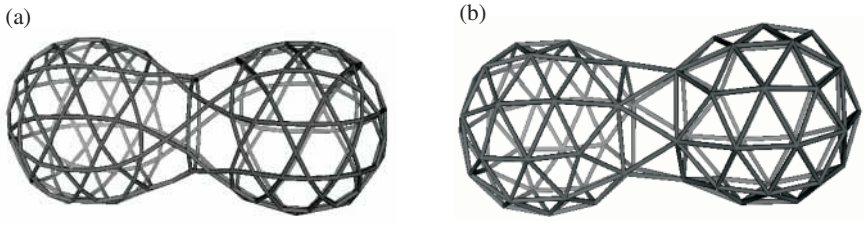

Figure 8. The medial (a) and the dual (b) of the C_{140}aa dimer.

planarity in the junction zone was found. Note that the enantiomer pairs have one and the same heat of formation.

Compared to the sp^3 dimers, the majority of sp^2 peanut dimers show a lower heat of formation (*i.e.*, a more relaxed structure) and only two distinct structures (Table VI, entries 9–11) are energetically higher than the most stable sp^3 structure. However, the HOMO-LUMO gap (a measure of kinetic stability) is higher for the sp^3 structures (the gap for the [6,6] adduct is 5.873 eV). Which, the heat of formation or the gap, will be dominant in the balance of factors that lead to one or another structure, remains a question.

CONCLUSIONS

All the sp^2 peanut dimers of $D_{5h}C_{70}$ have been constructed and characterized as topology and energetics.

The topology of the isomers was monitored by a cyclic permutation bond table. Semiempirical calculations supplied the same heat of formation for the enantiomer pairs. The classes of equivalence for the vertices, edges and faces of the studied peanut dimers were calculated by using two topological indices (as equivalence criteria) derived on the layer matrices of the associated graphs. They were calculated for the parent fullerenes, their medials and duals.

TABLE VI. Heat of formation, the band gap and point group symmetry for the C_{140} isomers

	Molecule	HF/kcal mol^{-1}	Band gap/eV	Symmetry
1	aa	11.768	5.136	D_{5d}
2	bb	11.882	4.446	C_2
3	bf	11.882	4.446	C_2
4	bc	11.938	4.083	C_2
5	bg	11.938	4.082	C_2
6	be	11.976	3.978	C_1
7	bd	11.976	3.978	C_1
8	dd	12.021	4.682	C_2
9	di	12.021	4.682	C_2
10	ce	12.082	5.747	C_{2h}
11	cf	12.082	5.752	C_2
12	cd	12.082	5.752	C_2
13	cc	12.084	5.739	C_2
14	cg	12.084	5.739	C_2
15	dh	12.092	4.671	C_2
16	de	12.092	4.671	C_2
17	df	12.100	4.624	C_2
18	dg	12.100	4.624	C_2
19	eg	12.705	4.512	D_2
20	ee	12.705	4.512	D_2
21	ef	12.924	2.119	D_2

The dimerization reaction of fullerenes clearly involves more than one dimeric species: sp^3 adduct, sp^2 peanut and sp^2 tubulene. Semiempirical calculations showed a decrease in the heat of formation along the presented reaction pathway. With the above results in mind, revisiting of the experimental data appears to be a real demand.

REFERENCES

1. H. Kroto, *Fullerene Sci. Technol.* **2** (1994) 333–342.
2. R. B. King, *Croat. Chem. Acta* **73** (2000) 993–1015.
3. H. Hosoya and Y. Tsukano, *Fullerene Sci. Technol.* **2** (1994) 381–393.
4. H. Zorc, Lj. P. Tolić, S. Martinović, and D. Srzić, *Fullerene Sci. Technol.* **2** (1994) 471–480.
5. F. Diedrich and C. Thilgen, *Science* **271** (1996) 317–323.
6. I. S. Neretin, K. A. Lyssenko, M. Yu. Antipin, Yu. L. Slovokhotov, O. V. Boltalina, P. A. Troshin, A. Yu. Lukonin, L. N. Sidorov, and R. Taylor, *Angew. Chem., Int. Ed. Engl.* **39** (2000) 3273–3276.
7. W. Qian and Y. Rubin, *Angew. Chem., Int. Ed. Engl.* **39** (2000) 3133–3137.
8. K. Lee, Ch. H. Lee, H. Song, J. T. Park, H. Y. Chang and M.-G. Choi, *Angew. Chem., Int. Ed. Engl.* **39** (2000) 1801–1804.
9. Y. D. Gao and W. C. Herndon, *J. Am. Chem. Soc.* **115** (1993) 8459–8460.
10. P. W. Fowler, T. Heine, D. E. Manolopoulos, D. Mitchell, G. Orlandini, R. Schmidt, G. Seiferth, and F. Zerbetto, *J. Phys. Chem.* **100** (1996) 6984–6991.
11. A. Müller, P. Kögerler, and Ch. Kuhlmann, *Chem. Commun.* (1999) 1347–1358.
12. S. Lebedkin, W. E. Hull, A. Soldatov, B. Renker and M. M. Kappes, *J. Phys. Chem. B* **104** (2000) 4101–4110.
13. P. W. Fowler, D. Mitchell, R. Taylor, and G. Seifert, *J. Chem. Soc., Perkin Trans. 2* (1997) 1901–1905.
14. S. Lebedkin, A. Gromov, S. Giesa, R. Gleiter, B. Renker, H. Rietschel, and W. Krätschmer, *Chem. Phys. Lett.* **285** (1998) 210–215.
15. D. L. Strout, R. L. Murry, C. Xu, W. C. Eckhoff, G. K. Odom, and G. E. Scuseria, *Chem. Phys. Lett.* **214** (1993) 576–582.
16. Y. Zhao, B. I. Yakobson, and R. E. Smalley, *Phys. Rev. Lett.* **88** (2002) 185501(4).
17. Y. Zhao, R. E. Smalley, and B. I. Yakobson, *Phys. Rev. B* **66** (2002) 195409(9).
18. K. Komatsu, K. Fujiwara, and Y. Murata, *Chem. Commun.* (2000) 1583–1584.
19. A. J. Stone and D. J. Wales, *Chem. Phys. Lett.* **128** (1986) 501–503.
20. L. Euler, *Comment. Acad. Sci. I. Petropolitanae* **8** (1736) 128–140.
21. D. J. Struik, *Classical Differential Geometry*, Dover Publications, New York, 1988.
22. M. Ştefu and M. V. Diudea, CageVersatile, v.1.1, »Babeş-Bolyai« University, 2003.
23. R. C. Haddon, *J. Am. Chem. Soc.* **112** (1990) 3385–3389.
24. R. C. Haddon and K. Raghavachari, in: W. E. Billups and M. A. Ciufolini, *Buckminsterfullerenes*, VCH, 1993, pp. 185–215.
25. R. C. Haddon and S.-Y. Chow, *J. Am. Chem. Soc.* **120** (1998) 10494–10496.
26. R. C. Haddon, *J. Phys. Chem. A* **105** (2001) 4164–4165.
27. M. V. Diudea and O. Ursu, *Indian J. Chem., Sect. A* **41** (2003) 1283–1294.
28. M. V. Diudea, P. E. John, A. Graovac, M. Primorac, and T. Pisanski, *Croat. Chem. Acta* **76** (2003) 153–159.
29. HyperChem™, Release 4.5 for SGI, © 1991–1995, HyperCube, Inc.

SAŽETAK

C_{70} dimeri – energetika i topologija

Csaba L. Nagy, Monica Stefu, Mircea V. Diudea, Andreas Dress i Achim Müller

Studirani su svi sp^2 dimerni fulereni kikirikijevoga oblika koji su izvedeni iz C_{70} fulerena simerije D_{5h}. Konstrukcija ovih izomera praćena je cikličkom permutacijom veza u zoni povezivanja dviju kapa koje su nastale uklanjanjem poligona iz C_{70} fulerena. Lokalna zakrivljenost je izračunana pomoću kutnih defekata i energije napetosti. Topologijske ekvivalencijske klase konstitutivnih podstruktura su numerički izražene pomoću topologijskoga indeksa izvornih kaveza, njihovih medijala i duala. Prikazana je u detalje transformacija od C_{70}, preko sp^3 dimera, sp^2 dimera kikirikijevoga oblika do odgovarajućega tubulena. Semiempirijski računi su pokazali da toplina formacije raste monotono duž spomenute transformacije.